SCIENTIFIC COMMITTEE
TWENTY-FIRST REGULAR SESSION

Nuku'alofa, Tonga
13-21 August 2025

Ecosystem and climate indicators of the western and central Pacific Ocean

WCPFC-SC21-2025/EB-IP-01

30th July 2025

SPC-OFP[1], CSIRO[2], MOi[3], IRD[4]

[1] Oceanic Fisheries Programme (OFP), Pacific Community (SPC), Noumea, New Caledonia.

[2] Environment Research Unit, CSIRO, Hobart, Australia.

[3] Mercator Oceans International, Toulouse, France.

[4] Institut de Recherche pour le Développement, MARBEC (Sete, France), ENTROPIE (Noumea, New Caledonia).

Table of contents

Executive Summary

This Working Paper updates SC21 on progress regarding development of a climate and ecosystem indicators report for the western and central Pacific Ocean (WCPO). We report that a workshop was successfully held in Suva, Fiji 25-26th November 2024 that brought collaborators together from a range of organisations. Those collaborators have contributed to the development of a workplan and candidate indicators presented in this report.

Substantial progress on candidate indicators has been achieved with a selection of these being prepared for inclusion in the “Overview of Fisheries and Stock Status” provided by the SSP to the Commission. Candidate climate indicators are now divided into three categories: (1) those that indicate change in the broad oceanography of the WCPO (i.e. climatological); (2) those that indicate change in key oceanographic features (i.e. warm pool); and (3) those that indicate direct impact on the fishery (both physical and bio-chemical). This report provides a format for the presentation of the indicators and a full description of each in the appendix. The discussion details whether these indicators meet the established screening criteria.

Recommendations

SC21 is invited to:

- note the progress made on the exploration, development and testing of candidate ecosystem and climate indicators for the WCPO.
- note this updated climate and ecosystem indicators report and the preparations to include these in the “Overview of Fisheries and Stock Status” provided by the SSP to the Commission.

Introduction

Changes in climate, both natural and anthropogenic forced, impact marine ecosystems and their associated fisheries (Antão *et al.,* 2020; Hoegh-Guldberg and Bruno, 2010; Pecl *et al.,* 2017; Poloczanska *et al.,* 2013). This includes impacts such as shifts in the ranges of species and ecosystems (Pecl *et al.,* 2017; Pinsky *et al.,* 2020), changes in species physiology (Agarwal *et al.,* 2024), and in community compositions (Johnson *et al.,* 2011; Poloczanska *et al.,* 2016, 2013). However, how these climate-induced impacts are manifesting themselves in individual species, ecosystems and fisheries are varied (Garciá Molinos *et al.,* 2017).

In response to climate change, fisheries administrations are increasingly looking at ways to monitor and adapt to its effects (Taylor and Walter, 2024). Within tuna regional fisheries management organisations (tRFMOs), ecosystem and climate indicator reports are now being regularly produced to monitor environmental conditions and to track if any underlying shifts in ecosystems, fisheries or species of interest are occurring (Griffiths and Fuller, 2019; Juan-Jordá *et al.,* 2018; SPC, 2023).

The WCPFC-SC has been exploring candidate ecosystem and climate indicators for the WCPO since SC15 (Allain *et al.,* 2021, 2020; Anon, 2015; Juan-Jordá *et al.,* 2019; SPC, 2024, 2023, 2022). Candidate indicators produced thus far have generally been empirical in nature, such as summarising catch and effort location, key environmental variables (e.g. sea surface temperature, ENSO events), and tuna biology (e.g. mean length of catch).

An expert workshop and member consultations were undertaken following SC20 recommendations to identify (and confirm the merits of) candidate indicators. In addition to endorsing the criteria for candidate indicator selection, splitting climate indicators into three broad categories was preferred: (1) those that indicate change in the broad oceanography of the WCPO (i.e. climatological); (2) those that indicate change in key oceanographic features (e.g. warm pool); and (3) those that indicate direct impact on the fishery (both physical and bio-chemical). Where feasible, indicators amenable to seasonal forecast and/or quantifying climate change effects should be developed to maximise their utility for the business of the WCPFC. Similarly, candidate indicators that integrate across several physical and/or bio-geo-chemical attributes is desirable (e.g. water temperature anomalies can be prepared to integrate changes in ocean heat and current). The workshop also concluded that rather than report to WCPFC annually on all candidate indicators, it would be more appropriate to report only those that inform the Commission of change which may vary from year to year. The SSP should seek advice from the SC to determine those that are included in the report to the Commission in each year.

Current candidate indicators are listed in Table 1. Selection and testing criteria for candidate indicators are listed in Appendix 1. Criteria to guide the data requirements for indicators have been provided following consultation at and after the expert workshop. Background information for each candidate indicator and evaluation against the selection criteria is provided in Appendix 2.

Discussion

This report presents the continued development and exploration of ecosystem and climate indicators for the WCPFC. The process of developing and selecting indicators is ongoing and is likely to evolve over time. Several new ocean climate indicators are presented to provide a more complete outlook of the state of oceanographic features of the WCPO. Two fishery indicators explored in previous reports were also updated and further examined herein. Although providing information and trends on WCPFC fisheries over time, underlying and inherent variability in these indicators likely renders them unresponsive as a climate indicator.

The ocean indicators presented monitor ocean variability and change, and will also be able to provide a comparison against climate models used for management decisions going forward. The science and databases used to produce these ocean indicators are readily available and updated regularly from the global ocean observing and satellite systems and international data product producers. However, recent changes in investment by some of the global partners in ocean monitoring may result in some loss in capability. As a result, the availability of some products may become limited into the future.

As gridded data products are predominately used, these indicators can be scaled to regional and sub-regional levels for the WCPO. This is needed because the WCPO is a large and complex region and how the climate and ocean interact, and how they will be impacted by ongoing climate change, will be variable meaning signals of change can be masked when examined at the basin scale.

For the fishery indicators explored here, it is not clear that either would be able to identify an underlying climate signal and therefore may not meet criteria four in relation to being responsive to climate and fishing pressure-related changes (Table 1). This is due to the fishery dependent nature of these indicators and their input data, making it difficult to disentangle a range of other variables (e.g. fishing strategy, data collection programs, flag) that influence these indicators.

At SC19, three candidate indicators were proposed including ENSO variability, ocean productivity, and warm pool area (SPC, 2023). These were found to meet all criteria except for criteria seven which relates to the ability of the indicator to be scalable to national and sub-regional scales. Several potential ocean indicators presented in previous SC reports including sea surface temperature, warm pool volume (or size), and primary productivity (chlorophyll-a concentration) have also been updated and modified herein, using different observational data products and looking at them with renewed focus. As part of this, several of these indicators have been explored at regional and national scales to address previous limitations.

SC21 is invited to note the progress made on the exploration, development and testing of candidate ecosystem and climate indicators for the WCPO. Since SC20:

- A successful workshop was held in Suva, Fiji in November 2024.
- Several new candidate indicators have been developed, and several proposed fishery indicators have been further explored and tested against the screening criteria.

Table 1. Candidate Indicators and recommendation for reporting.

Name	Descriptor	Comment	2025 WCPFC Report
WCPFC Climatological Indicators			
Water temperature	SST anomaly Ocean Heat Content Depth of Isotherms	Sea surface temperature (SST) trends are spatially variable, with warming in some areas and cooling in others. More appropriate to present by oceanographic feature/region.	Meets selection criteria but more informative to present by oceanographic region
Interdecadal Pacific Oscillation (IPO)	Tripole index	IPO is currently in a neutral phase and potentially shifting to a positive (warming) phase. WCPFC should monitor as it will influence trends.	Meets selection criteria and aids interpretation of warming trends
El Nino Southern Oscillation (ENSO)	Nino 3.4 index	Well established driver of equatorial Pacific fishery dynamics. WCPFC should monitor as it influences trends.	Meets selection criteria and aids interpretation of interannual trends
Marine heatwaves	Intensity Frequency Area impacted	More appropriate to present by oceanographic feature/region given the spatial variability.	Meets selection criteria but more informative to present by oceanographic region
Oceanographic Feature/region			
Western Pacific warm pool	Area of 29°C Area of 31°C	Main feature of the western equatorial Pacific and projected in climate models to be increasing. Area of 31°C isotherm indicates threshold for declining skipjack larval habitat.	Meets selection criteria
Nino 3.4 area	ENSO intensity ENSO frequency Depth of Isotherms	Reported increasing intensity of El Nino events should be monitored. Appendix 2 detects patterns of a deepening of the isotherms in this area and immediately to the south.	Meets selection criteria
North Pacific gyre	SST anomaly	Patterns of long-term warming detected in this area.	Meets selection criteria
South Pacific gyre	SST anomaly	Patterns of long-term warming detected in this area.	Meets selection criteria
Marine heat wave (MHW) regions	Intensity Frequency	Patterns of increasing frequency and intensity of MHWs detected in historical records.	Meets selection criteria

	Area impacted		
Fishery Related			
	Oxygen	Discrimination between seasonal, interannual and long term variability not yet complete.	Under development
	Chlorophyll-a concentration	Discrimination between seasonal, interannual and long term variability not yet complete.	Under development
	Acidification		Under development
	Centre of gravity of purse seine catch and effort	Climate signal not detected (see Appendix 2).	Does not currently meet selection criteria
	Length composition of tunas	Climate signal not detected (see Appendix 2).	Does not currently meet selection criteria
	SEAPODYM spawning	Available once new reference models for each species are fully assessed.	Under development
Ecosystem			
	Mean condition of catch	SC 18 did not detect sufficient sensitivity.	Does not currently meet selection criteria, data limitations
	Bycatch trends	Separate SC paper.	Meets selection criteria
	Redistribution of species	Available for testing in 2026.	Under development
	Ecosystem traits index	Available for testing in 2026.	Under development
	Impacts on food webs (LTML)	Available once new SEAPODYM reference models for each species are fully assessed.	Under development

References

Agarwal, D., Shanmugam, S.A., Kathirvelpandian, A., Eswaran, S., Rather, M.A., Rakkannan, G., 2024. Unraveling the impact of climate change on fish physiology: a focus on temperature and salinity dynamics. Journal of Applied Ichthyology, 2024(1), p.5782274.

Allain, V., Hare, S., Macdonald, J., Machful, P., Nicol, S., Phillips, J.S., Portal, A., Vidal, T., Williams, P., 2021. WCPO Ecosystem and Climate Indicators from 2000 to 2020. WCPFC Scientific Committee 17th Regular Session, WCPFC-SC17-2021/EB-IP-09, Online.

Allain, V., Macdonald, J., Nicol, S., Phillips, J.S., Vourey, E., 2020. Ecosystem and climate indicators for consideration within the WCPO. WCPFC Scientific Committee 16th Regular Session, WCPFC-SC16-2020/EB-IP-07, Online.

Anon, 2015. Summary Report: Commission for the Conservation and Management of Highly Migratory Fish Stocks in the Western and Central Pacific Ocean. WCPFC Scientific Committee 11th Regular Session, Pohnpei.

Antão, L.H., Bates, A.E., Blowes, S.A., Waldock, C., Supp, S.R., Magurran, A.E., Dornelas, M., Schipper, A.M., 2020. Temperature-related biodiversity change across temperate marine and terrestrial systems. Nat Ecol Evol. https://doi.org/10.1101/841833

Ashida, H., 2020. Spatial and temporal differences in the reproductive traits of skipjack tuna Katsuwonus pelamis between the subtropical and temperate western Pacific Ocean. Fish Res 221, 105352. https://doi.org/10.1016/j.fishres.2019.105352

Bell, J.D., Senina, I., Adams, T., Aumont, O., Calmettes, B., Clark, S., Dessert, M., Gehlen, M., Gorgues, T., Hampton, J., Hanich, Q., Harden-Davies, H., Hare, S.R., Holmes, G., Lehodey, P., Lengaigne, M., Mansfield, W., Menkes, C., Nicol, S., Ota, Y., Pasisi, C., Pilling, G., Reid, C., Ronneberg, E., Gupta, A. Sen, Seto, K.L., Smith, N., Taei, S., Tsamenyi, M., Williams, P., 2021. Pathways to sustaining tuna-dependent Pacific Island economies during climate change. Nat Sustain 4, 900–910. https://doi.org/10.1038/s41893-021-00745-z

Bopp, L., Aumont, O., Cadule, P., Alvain, S., Gehlen, M., 2005. Response of diatoms distribution to global warming and potential implications: A global model study. *Geophysical Research Letters*, *32*(19), n/a-n/a. https://doi.org/10.1029/2005GL023653

Buchanan, P. J., Aumont, O., Bopp, L., Mahaffey, C., Tagliabue, A., 2021. Impact of intensifying nitrogen limitation on ocean net primary production is fingerprinted by nitrogen isotopes. *Nature Communications*, *12*(1), 6214. https://doi.org/10.1038/s41467-021-26552-w

Buchanan, P. J., Pierella Karlusich, J. J., Tuerena, R. E., Shafiee, R., Woodward, E. M. S., Bowler, C., Tagliabue, A., 2025. Oceanic enrichment of ammonium and its impacts on phytoplankton community composition under a high-emissions scenario. EGUsphere preprint, https://doi.org/10.5194/egusphere-2024-3639

Capotondi, A., McGregor, S., McPhaden, M.J., Cravatte, S., Holbrook, N.J., Imada, Y., Sanchez, S.C., Sprintall, J., Stuecker, M.F., Ummenhofer, C.C., Zeller, M., 2023. Mechanisms of tropical Pacific decadal variability. Nature Reviews Earth & Environment, 4(11), pp.754-769. https://doi.org/10.1038/s43017-023-00486-x

Duteil, O., Oschlies, A., Böning, C.W., 2018. Pacific Decadal Oscillation and recent oxygen decline in the eastern tropical Pacific Ocean. *Biogeosciences*, *15*(23), 7111–7126. https://doi.org/10.5194/bg-15-7111-2018

FAO, 2024. The State of World Fisheries and Aquaculture 2024 - Blue Transformation in action, The State of World Fisheries and Aquaculture 2024. FAO, Rome. https://doi.org/10.4060/cd0683en

Farley, J., Eveson, P., Krusic-Golub, K., Sanchez, C., Roupsard, F., Mckechnie, S., Nicol, S., Leroy, B., Smith, N., Chang, S.-K., 2017. Project 35: Age, growth and maturity of bigeye tuna in the western and central Pacific Ocean. WCPFC Scientific Committee 13th Regular Session, WCPFC-SC13-2017/ SA-WP-01, Rarotonga.

Fujioka, K., Aoki, Y., Tsuda, Y., Okamoto, K., Tsuchida, H., Sasaki, A., Kiyofuji, H., 2024. Influence of temperature on hatching success of skipjack tuna (Katsuwonus pelamis): Implications for spawning availability of warm habitats. J Fish Biol 105, 372–377. https://doi.org/10.1111/jfb.15767

Garciá Molinos, J., Burrows, M.T., Poloczanska, E.S., 2017. Ocean currents modify the coupling between climate change and biogeographical shifts. Sci Rep 7. https://doi.org/10.1038/s41598-017-01309-y

Ganachaud, A., Cravatte, S., Melet, A., Schiller, A., Holbrook, N.J., Sloyan, B.M., Widlansky, M.J., Bowen, M., Verron, J., Wiles, P. and Ridgway, K., 2014. The Southwest Pacific Ocean Circulation and Climate Experiment (SPICE) Report to CLIVAR SSG. 119, doi:10.1002/2013JC009678

Griffiths, S., Fuller, L., 2019. Ecosystem Considerations. Inter-American Tropical Tuna Commission, Scientific Advisory Committee Tenth Meeting, San Diego.

Hoegh-Guldberg, O., Bruno, J.F., 2010. The impact of climate change on the world's marine ecosystems. Science (1979). https://doi.org/10.1126/science.1189930

Hong, Z., Long, D., Li, X., Wang, Y., Zhang, J., Hamouda, M. A., Mohamed, M.M., 2023. A global daily gap-filled chlorophyll-a dataset in open oceans during 2001-2021 from multisource information using convolutional neural networks. Earth System Science Data, 15(12), 5281–5300. https://doi.org/10.5194/essd-15-5281-2023

Huang, B., Liu, C., Banzon, V., Freeman, E., Graham, G., Hankins, B., Smith, T., Zhang, H., 2021. Improvements of the Daily Optimum Interpolation Sea Surface Temperature (DOISST) Version 2.1. *J. Climate*, 34, 2923–2939, https://doi.org/10.1175/JCLI-D-20-0166.1.

Ito, T., Deutsch, C., 2013. Variability of the oxygen minimum zone in the tropical North Pacific during the late twentieth century. *Global Biogeochemical Cycles*, *27*(4), 1119–1128. https://doi.org/10.1002/2013GB004567

Johnson, C.R., Banks, S.C., Barrett, N.S., Cazassus, F., Dunstan, P.K., Edgar, G.J., Frusher, S.D., Gardner, C., Haddon, M., Helidoniotis, F., Hill, K.L., Holbrook, N.J., Hosie, G.W., Last, P.R., Ling, S.D., Melbourne-Thomas, J., Miller, K., Pecl, G.T., Richardson, A.J., Ridgway, K.R., Rintoul, S.R., Ritz, D.A., Ross, D.J., Sanderson, J.C., Shepherd, S.A., Slotwinski, A., Swadling, K.M., Taw, N., 2011. Climate change cascades: Shifts in oceanography, species' ranges and subtidal marine community dynamics in eastern Tasmania. J Exp Mar Biol Ecol. https://doi.org/10.1016/j.jembe.2011.02.032

Juan-Jordá, M., Murua, H., Apostolaki, P., Lynam, C., Rodriguez, A., Barrionuevo, J., Abascal, F., Coelho, R., Todorovic, S., Billet, N., Uyarra, M., Andonegi, E., Lopez, J., 2019. Selecting ecosystem indicators for fisheries targeting highly migratory species: An EU project to advance the operationalization of the EAFM in ICCAT and IOTC. WCPFC Scientific Committee 15th Regular Session, WCPFC-SC15-2019/EB-WP-12, Pohnpei.

Juan-Jordá, M.J., Murua, H., Arrizabalaga, H., Hanke, A., 2018. A template for an indicator-based ecosystem report card for ICCAT. International Commission for the Conservation of Atlantic Tunas, SCRS/2017/140, Sci. Pap. ICCAT.

Kwiatkowski, L., Torres, O., Bopp, L., Aumont, O., Chamberlain, M., Christian, J.R., Dunne, J.P., Gehlen, M., Ilyina, T., John, J. G., Lenton, A., Li, H., Lovenduski, N. S., Orr, J. C., Palmieri, J., Santana-Falcón, Y., Schwinger, J., Séférian, R., Stock, C. A., Ziehn, T., 2020. Twenty-first century ocean warming, acidification, deoxygenation, and upper-ocean nutrient and primary production decline from CMIP6 model projections. *Biogeosciences*, *17*(13), 3439–3470. https://doi.org/10.5194/bg-17-3439-2020

Lal, S., Cravatte, S., Menkes, C., Macdonald, J., LeGendre, R., Mangolte, I., Dutheil, C., Holbrook, N., Nicol, S. (*preprint*). Characterization of Past Marine Heatwaves around South Pacific Island Countries: What really matters? *EGUsphere,* https://doi.org/10.5194/egusphere-2025-3281.

Lehodey, P., Senina, I., Calmettes, B., Hampton, J., Nicol, S., 2013. Modelling the impact of climate change on Pacific skipjack tuna population and fisheries. Clim Change 119, 95–109. https://doi.org/10.1007/s10584-012-0595-1

Matear, R.J., Chamberlain, M.A., Sun, C., Feng, M., 2015. Climate change projection for the western tropical Pacific Ocean using a high-resolution ocean model: Implications for tuna fisheries. *Deep Sea Research Part II: Topical Studies in Oceanography*, *113*, 22–46. https://doi.org/10.1016/j.dsr2.2014.07.003

Oschlies, A., Brandt, P., Stramma, L., Schmidtko, S., 2018. Drivers and mechanisms of ocean deoxygenation, Nat. Geosci., 11, 467–473, https://doi.org/10.1038/s41561-018-0152-2.

Pecl, G.T., Araújo, M.B., Bell, J.D., Blanchard, J., Bonebrake, T.C., Chen, I.-C., Clark, T.D., Colwell, R.K., Danielsen, F., Evengård, B., Falconi, L., Ferrier, S., Frusher, S., Garcia, R.A., Griffis, R.B., Hobday, A.J., Janion-Scheepers, C., Jarzyna, M.A., Jennings, S., Lenoir, J., Linnetved, H.I., Martin, V.Y., McCormack, P.C., McDonald, J., Mitchell, N.J., Mustonen, T., Pandolfi, J.M., Pettorelli, N., Popova, E., Robinson, S.A., Scheffers, B.R., Shaw, J.D., Sorte, C.J.B., Strugnell, J.M., Sunday, J.M., Tuanmu, M.N., Vergés, A., Villanueva, C., Wernberg, T., Wapstra, E., Williams, S.E., 2017. Biodiversity redistribution under climate change: Impacts on ecosystems and human well-being. Science (1979). https://doi.org/10.1126/science.aai9214

Pinsky, M.L., Selden, R.L., Kitchel, Z.J., 2020. Climate-Driven Shifts in Marine Species Ranges: Scaling from Organisms to Communities. Ann Rev Mar Sci 12, 153–179. https://doi.org/10.1146/annurev-marine-010419

Poloczanska, E.S., Brown, C.J., Sydeman, W.J., Kiessling, W., Schoeman, D.S., Moore, P.J., Brander, K., Bruno, J.F., Buckley, L.B., Burrows, M.T., Duarte, C.M., Halpern, B.S., Holding, J., Kappel, C. V., O'Connor, M.I., Pandolfi, J.M., Parmesan, C., Schwing, F., Thompson, S.A., Richardson, A.J., 2013. Global imprint of climate change on marine life. Nat Clim Chang 3, 919–925. https://doi.org/10.1038/nclimate1958

Poloczanska, E.S., Burrows, M.T., Brown, C.J., Molinos, J.G., Halpern, B.S., Hoegh-Guldberg, O., Kappel, C. V., Moore, P.J., Richardson, A.J., Schoeman, D.S., Sydeman, W.J., 2016. Responses of marine organisms to climate change across oceans. Front Mar Sci. https://doi.org/10.3389/fmars.2016.00062

R Core Team, 2024. R: A language and environment for statistical computing.

Renard D., Bez N., Desassis N., Beucher H., Ors F., Freulon X., 2023. RGeostats: The Geostatistical R Package. Version: [14.0.10'] http://cg.ensmp.fr/rgeostats.

Roemmich, D., Gilson, J., 2009. The 2004–2008 mean and annual cycle of temperature, salinity, and steric height in the global ocean from the Argo Program. Progress in oceanography, 82(2), pp.81-100.

Senina, I., Sibert, J., Lehodey, P., 2008. Parameter estimation for basin-scale ecosystem-linked population models of large pelagic predators: Application to skipjack tuna. Prog Oceanogr 78, 319–335. https://doi.org/10.1016/j.pocean.2008.06.003

Schaefer, K.M., Fuller, D.W., 2010. Vertical movements, behavior, and habitat of bigeye tuna (Thunnus obesus) in the equatorial eastern Pacific Ocean, ascertained from archival tag data. *Marine Biology*, *157*(12), 2625–2642. https://doi.org/10.1007/s00227-010-1524-3

Schaefer, K.M., Fuller, D.W., 2007. Vertical movement patterns of skipjack tuna (Kotsuwonus pelamis) in the eastern equatorial Pacific Ocean, as revealed with archival tags. *Fishery Bulletin*, vol. 105, no. 3, pp. 379. *Gale Academic OneFile*, link.gale.com/apps/doc/A169086817/AONE?u=anon~4400fa6c&sid=googleScholar&xid=c6e4b8a9. Accessed 14 July 2025.

Schaefer, K.M., Fuller, D.W., Block, B.A., 2009. Vertical Movements and Habitat Utilization of Skipjack (Katsuwonus pelamis), Yellowfin (Thunnus albacares), and Bigeye (Thunnus obesus) Tunas in the Equatorial Eastern Pacific Ocean, Ascertained Through Archival Tag Data. In: Nielsen, J.L., Arrizabalaga, H., Fragoso, N., Hobday, A., Lutcavage, M., Sibert, J. (eds) Tagging and Tracking of Marine Animals with Electronic Devices. Reviews: Methods and Technologies in Fish Biology and Fisheries, vol 9. Springer, Dordrecht. https://doi.org/10.1007/978-1-4020-9640-2_8

Schaefer, K.M., Fuller, D.W., Block, B.A., 2011. Movements, behavior, and habitat utilization of yellowfin tuna (Thunnus albacares) in the Pacific Ocean off Baja California, Mexico, determined from archival tag data analyses, including unscented Kalman filtering. Fisheries Research, 112(1–2), 22–37. https://doi.org/10.1016/j.fishres.2011.08.006

Schmidtko, S., Stramma, L., Visbeck, M., 2017. Decline in global oceanic oxygen content during the past five decades, Nature, 542, 335–339, https://doi.org/10.1038/nature21399, 2017.

Silsbe, G.M., Fox, J., Westberry, T.K., Halsey, K.H., 2025. Global declines in net primary production in the ocean color era. *Nature Communications*, *16*(1), 5821. https://doi.org/10.1038/s41467-025-60906-y

Sharp, J. D., Fassbender, A. J., Carter B. R., Johnson, G. C., Schultz, C., Dunne, J. P., 2023. GOBAI-O_2: temporally and spatially resolved fields of ocean interior dissolved oxygen over nearly 2 decades. Earth System Science Data, 15, 4481–4518, https://doi.org/10.5194/essd-15-4481-2023

Stramma, L., Schmidtko, S., 2021. Spatial and Temporal Variability of Oceanic Oxygen Changes and Underlying Trends, Atmos. Ocean, 59, 122–132, https://doi.org/10.1080/07055900.2021.1905601.

SPC, 2024. Ecosystem and climate indicators. Oceanic Fisheries Programme, Pacific Community, WCPFC Scientific Committee 20th Regular Session, WCPFC-SC20-2024/EB-WP-01, Manila.

SPC, 2023. Ecosystem and Climate Indicators. Oceanic Fisheries Programme, Pacific Community, WCPFC Scientific Committee Nineteenth Regular Session, WCPFC-SC19-2023/EB-WP-01, Koror.

SPC, 2022. Ecosystem and climate indicators. Oceanic Fisheries Programme, Pacific Community, WCPFC Scientific Committee 18th Regular Session, WCPFC-SC18-2022/EB-WP-01, Online.

Takano, Y., Ilyina, T., Tjiputra, J., Eddebbar, Y. A., Berthet, S., Bopp, L., Buitenhuis, E., Butenschön, M., Christian, J. R., Dunne, J. P., Gröger, M., Hayashida, H., Hieronymus, J., Koenigk, T., Krasting, J. P., Long, M. C., Lovato, T., Nakano, H., Palmieri, J., ... Yool, A., 2023. Simulations of ocean deoxygenation in the historical era: insights from forced and coupled models. *Frontiers in Marine Science*, *10*. https://doi.org/10.3389/fmars.2023.1139917

Tagliabue, A., Kwiatkowski, L., Bopp, L., Butenschön, M., Cheung, W., Lengaigne, M., Vialard, J., 2021. Persistent uncertainties in ocean net primary production climate change projections at regional scales raise challenges for assessing impacts on ecosystem services. *Frontiers in Climate*, *3*(November), 1–16. https://doi.org/10.3389/fclim.2021.738224

Taylor, N.G., Walter, J.F., 2024. Incorporating climate considerations into fisheries assessments and management advice at ICCAT. International Commission for the Conservation of Atlantic Tunas, SCRS/2024/081, Collect. Vol. Sci. Pap. ICCAT.

Wood, S.N., 2011. Fast stable restricted maximum likelihood and marginal likelihood estimation of semiparametric generalized linear models. J R Stat Soc Series B Stat Methodol 73, 3–36. https://doi.org/10.1111/j.1467-9868.2010.00749.

Appendix 1: Criteria for selecting candidate ecosystem and climate indicators

Process for adopting indicators

SC12 noted that developing a thorough understanding of how to interpret potential indicators, their appropriate reference levels and baselines, and how reliable they are for prediction were critical steps for indicator adoption by the WCPFC Scientific Committee (SC). Criteria for developing and testing candidate indicators has subsequently been proposed to the Scientific Committee:

Indicator Criteria	***Data Criteria***
1. *science and data based;*	• Data should be publicly available and be quantitative, specific, and preferably directly measurable or observable.
2. *characterize the states and trends of WCPFC marine ecosystems with respect to fishing activity and/or climate (including reference levels and baselines);*	• Data should be updated on a regular basis, preferably at least annually.
3. *reflect well-defined processes underlying fishing activity and fishery responses to climate;*	• Time-series used should be long-term (>10-years preferred).
4. *responsive to changes attributable to fishing pressure and climate (i.e. having minimal time-lags and capability to provide early warning);*	• Data should have appropriate and adequate spatial coverage.
5. *estimable on a routine basis with a historical data time-series available;*	• Data should have sufficient signal-to-noise ratio to estimate measurement, process uncertainty, and detect significant change.
6. *cost-effectiveness;*	• Explanation of the limits of data must be documented.
7. *scalable across national, sub-regional and regional scales;*	

8. *linked to existing WCPFC models and decision-making processes (for inclusion in MSE scenarios, validation of predictions and testing of model assumptions);*	
9. *can be routinely estimated by members without reliance on the Science Service Provider.*	

Appendix 2: Candidate Indicators

WCPFC Climatological Indicators: Water temperature

Rationale: Water temperature is influenced by a variety of factors, including solar radiation, wind patterns, ocean currents, and larger climate patterns like ENSO events. These drivers can cause both warming and cooling trends, and their interactions are complex, leading to differing trends throughout the WCPO. How water temperature patterns will change in the Pacific Ocean with global warming has world-wide implications such as regional changes in rainfall, where drought occurs, numbers of tropical cyclones, the rate of global mean warming, circulation patterns, ocean biogeochemistry, ocean productivity and distribution of organisms. For example, faster warming in the western Pacific than in the eastern Pacific is likely to result in the background tropical circulation becoming more La Nina-like (relatively cooler in the central/east Pacific and warmer in the western Pacific). However, if the east warms faster than the west in the future, the circulation across the tropical Pacific could become more El Nino-like (relatively warmer in the central/east Pacific and cooler in the western Pacific). Tracking both variability and long-term trends in water temperature throughout the WCPO will help identify any underlying climate-driven trends and any impact they may have on WCPFC fisheries. Sea surface temperature observation and ocean heat content are readily available measures of water temperature.

i. Sea-Surface Temperature (SST)

Description: SST was derived from the NOAA OISST product which combines in-situ ocean and satellite observations (Huang *et al.,* 2021). NOAA OISST data are available daily on a 0.25° degree resolution. The in-situ and satellite observations are interpolated onto a regular grid and objectively analysed to fill data gaps, providing consistent coverage across the study region. For OISST, the mean climatology is calculated for each grid cell over the entire timeseries with complete yearly data (1982-2024). The daily data are averaged for each calendar month and monthly anomalies are the difference of monthly SST from the mean climatology (1982-2024). Monthly SST and anomalies are then averaged over each region.

The spatial trends in SST and ocean heat content in the Pacific are diverse with differing rates of warming and cooling. To account for this variation and explore trends in SST in space and time the WCPO was divided into eight large sub-regions based on dominant ocean circulation features (Figure A2-1).

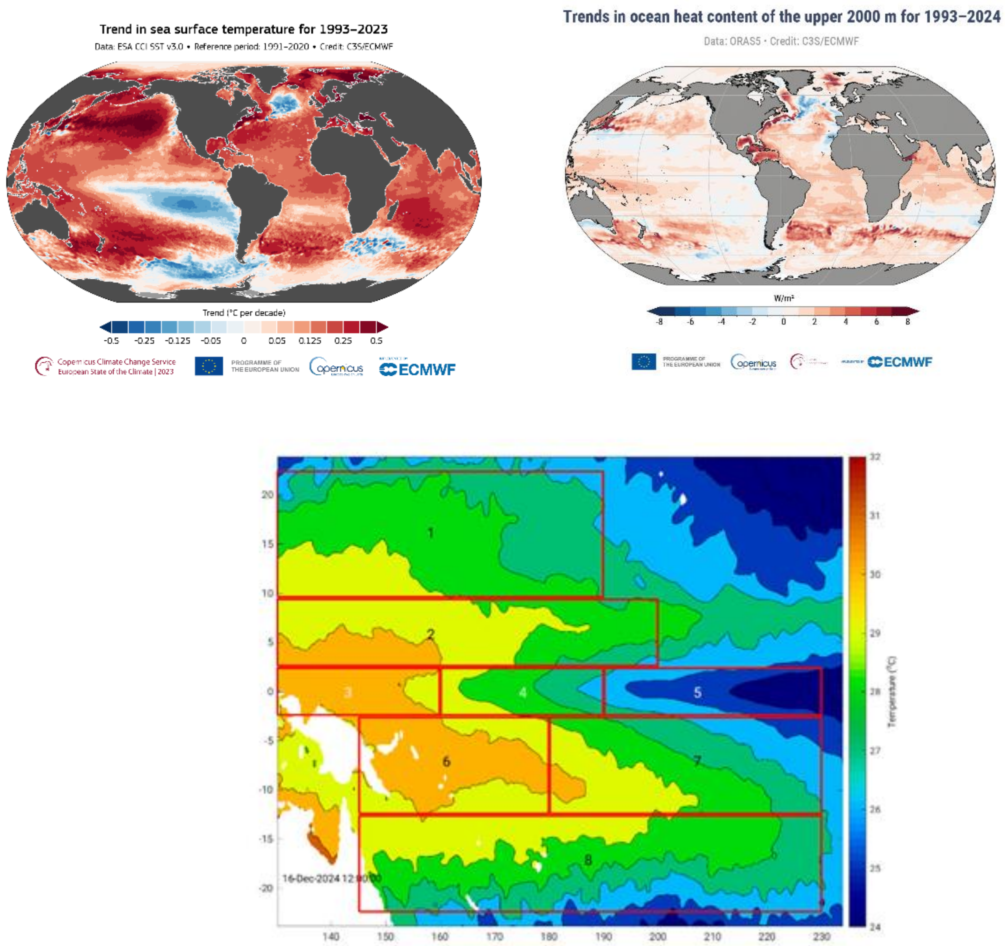

*Figure A2-1: **Upper Left Panel**: Trend in annual sea surface temperature anomalies (°C/decade) for the period 1993–2023. Data source: ESA SST CCI Analysis v3.0. Credit: ESACCI/EOCIS/UKMCAS and C3S/ECMWF. **Upper Right Panel**: Trend in the ocean heat content (W/m^2) of the upper 2000m for 1993–2024. Source: ORAS5. Credit: C3S/ECMWF. **Bottom Panel**: The eight western and central Pacific Ocean regions used to monitor sea surface temperature (SST) and its variability (figure shows monthly SST for December 2024). These regions are: Region 1: 22.5-9.5°N, 130-190°E; Region 2: 9.5-2.5°N, 130-200°E; Region 3: 2.5°N-2.5°S, 130-160°E; Region 4: 2.5°N-2. 5°S, 160-190°E; Region 5: 2.5°N-2.5°S, 190-230°E; Region 6: 2.5-12.5°S, 145-180°E; Region 7: 2.5-12.5°S, 180-230°E; Region 8: 12.5-22.5°S, 145-230°E.*

Status: Monthly SSTs and their anomaly relative to the climatological mean (1982-2024) are presented for the eight regions from September 1981 to March 2025. These figures show that SST in the northern and southern regions of the WCPO away from the equator between 22.5-12.5°N/S (Region 1 and 8), have a clear seasonal cycle. However, throughout 1981-2025 there is also evidence of an ocean warming trend overlain on this seasonal cycle (Figure A2-2 left panels). The anomaly in Region 1 has been in the higher range in recent years (2024 and 2023 are highlighted in the right panels of Figure A2-2).

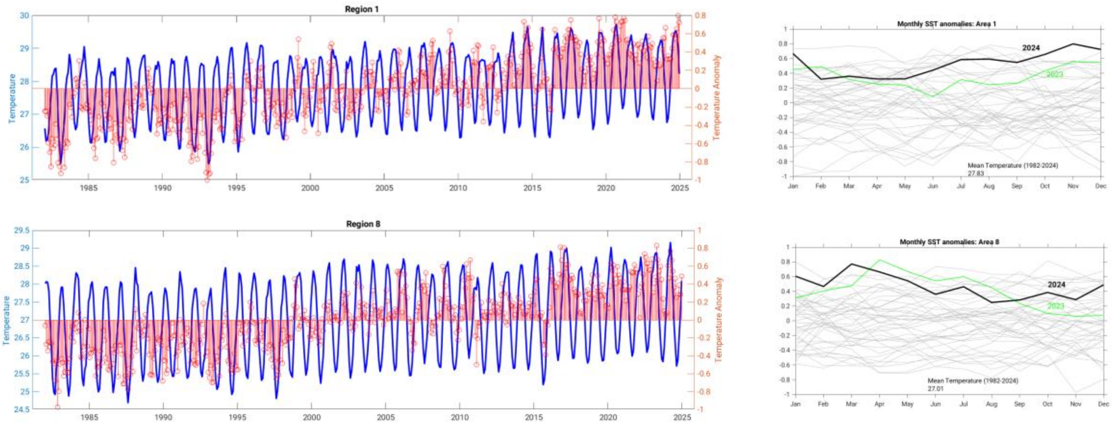

Figure A2-2: Monthly SST anomalies for Region's 1 and 8 relative to the climatological mean (1982-2024).

Closer to the equator in Regions 2 and 6 and in the western equatorial region (Region 3), the seasonal SST variability and warming trend has a superimposed interannual cycle of approximately 5-8 years of greater amplitude in temperature anomaly (Figure A2-3, left panels). 2024 was the hottest in the time series for Region's 3 and 6 (Figure A2-3, right panels).

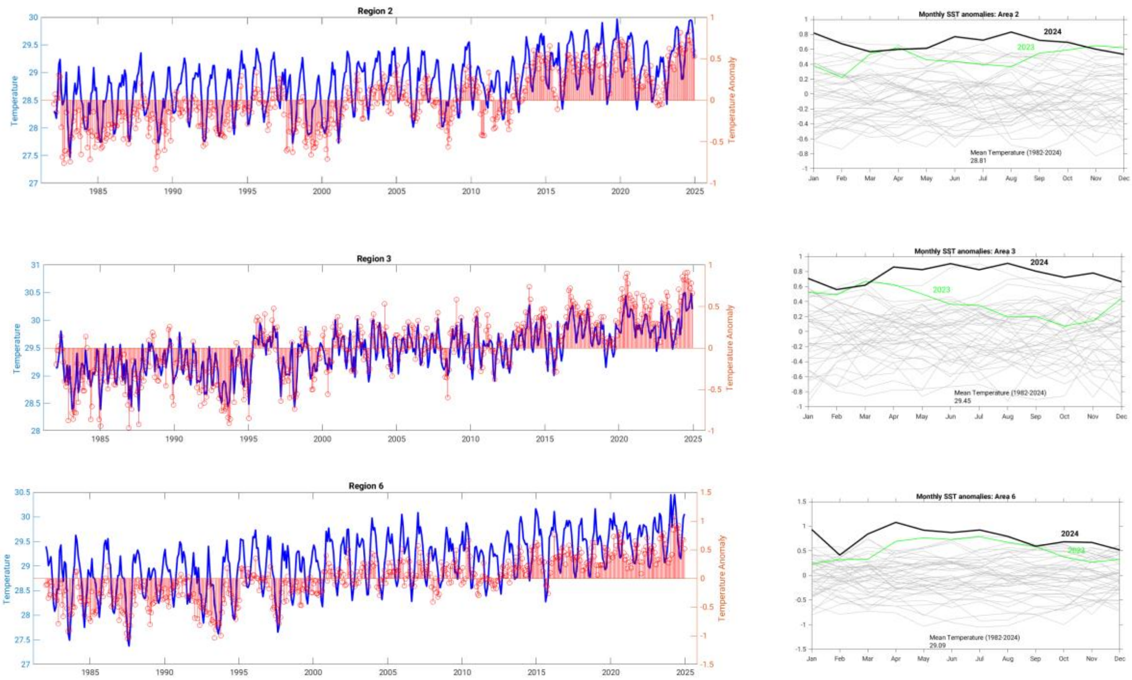

Figure A2-3: Monthly SST anomalies for Region's 2, 3 and 6 relative to the climatological mean (1982-2024).

The equatorial regions (Region 4 and 5) and the central Pacific (Region 7) between 2.5 °S and 12.5 °S, and east of 180°E show the largest SST fluctuations and variability due to the east-west movement of the warm pool along the equator and displacement of warm water off the equator (Figure A2-4). SST anomalies are predominately driven by ENSO events in Regions 4, 5, and 7 and are large (up to 2.7ºC), dominating any climate change trend that may be present.

Current evaluation is that SST anomalies meet all indicator selection criteria with trends identified in regions 1 and 8 the most informative for WCPFC.

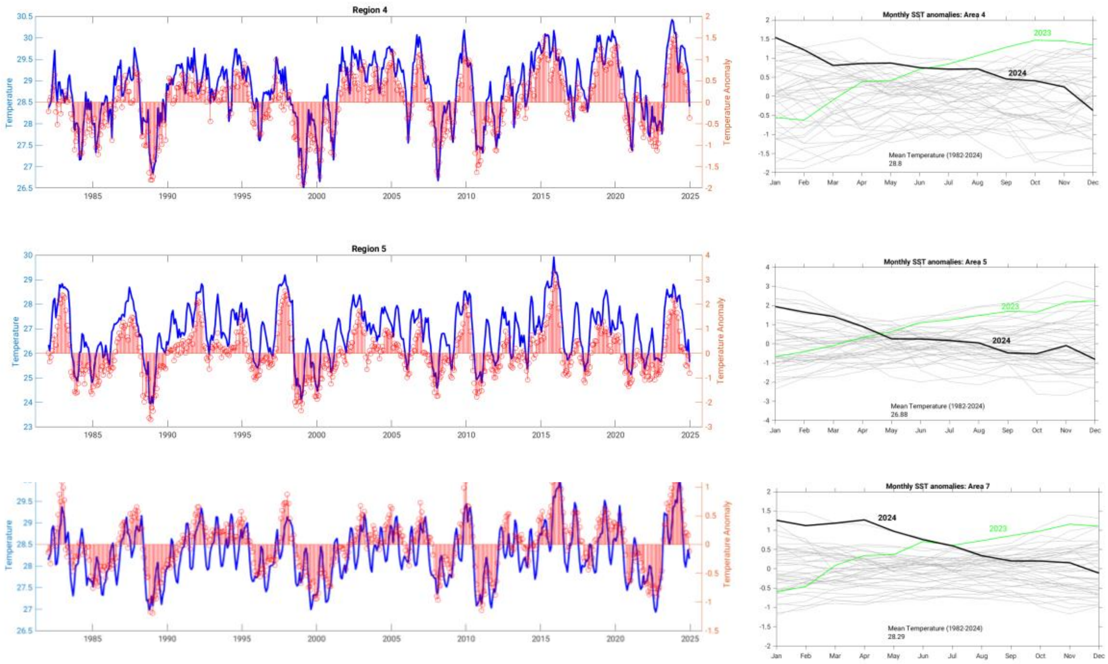

Figure A2-4: Monthly SST anomalies for Region's 4, 5 and 7 relative to the climatological mean (1982-2024).

ii. Depth of subsurface ocean isotherms

Description: Subsurface layers of constant temperature, called isotherms, are useful to delineate the boundaries between oceanographic regimes and understand the vertical structure of the water column. Isotherms can be used to monitor variability and change in key ocean currents, upper heat content and vertical mixing, which are influenced by a range of factors such as ENSO events. The 20ºC isotherm for example, is commonly used to delineate the boundary between warm, nutrient-poor waters close to the surface from deep, colder nutrient-rich waters. With the effects of climate change, the ocean is expected to absorb much of the heat. The depth of an isotherm is a measure of the upper ocean heat content – the deeper an isotherm the higher the heat content.

The data used is derived from the Roemmich and Gilson Argo monthly 0.25º latitude by longitude climatology to map the sub-surface ocean structure (Roemmich and Gilson, 2009). For each month, the depth of six isotherms (30, 28, 24, 20 ,15, 10ºC) was extracted at each grid cell of the climatology. This indicator is calculated from 2004 when the Argo network reached its global observational network density. To capture the north-south and west-east structure of the WCPO, four longitudes spanning the WCPO region have been selected (Figure A2-5).

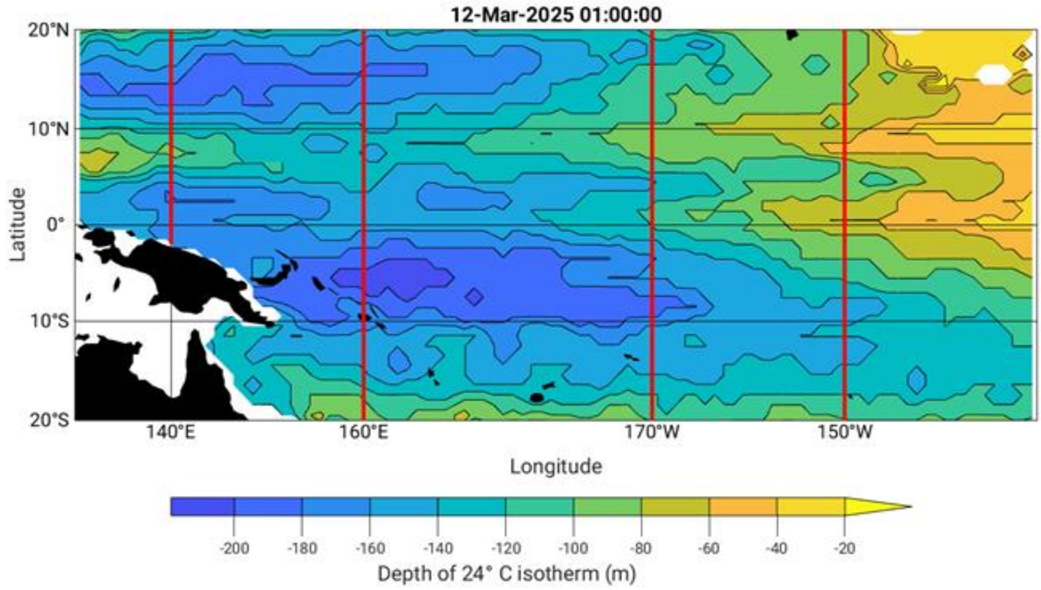

Figure A2-5: An example output of the depth of the 24°C isotherm in March 2025 throughout the western and central Pacific Ocean. The selected longitudes, 140°E, 160°E, 190°E (170°W), and 210°E (150°W) are identified by bold red lines. In March 2025, the depth of the 24°C isotherm varies from greater than 200m along approximately 5°S and 15°N, west of 170°W (190°E), and is shallower than 40m along the equator and northward east of 150°W (210°E). The deeper the isotherm, the warmer the upper ocean. Thus, the upper ocean is warmer both north and south of the equator west of 170°W (190°E), with a warmer upper ocean extending further east between 5°S to 15°S.

Status: The depth of the 24°C and 20°C isotherms for the four longitudes highlighted in Figure A2-5 are shown in Figure A2-6 and A2-7 (not shown are similar plots for the 15°C and 10°C isotherms). Isotherms are generally deeper off the equator with the maximum depth found between 5°S and 15°S. The depth of the 24°C isotherm moves southward in the central Pacific tracking the increased latitudinal size of the Subtropical Cell due to the increased strength of wind-driven divergence. Figure A2-6 and A2-7 show that the ocean heat content is greatest between 5°S and 15°S and has a strong seasonal cycle between 160°E and 170°W.

The latitudinal variations in the maximum depth of isotherms also shows an interannual cycle that is correlated with ENSO, particularly La Nina events at 160°E and 170°E for the 24°C isotherm. The variation in depth of the isotherm provides a measure of heat storage of the tropical Pacific and the latitudinal depth gradient of the isotherm provides an index of the strength of the subsurface currents vertical exchange between the surface and subsurface ocean. Current evaluation is that depth of subsurface isotherms meet all indicator selection criteria with trends identified most informative for WCPFC to monitor inter-annual patterns.

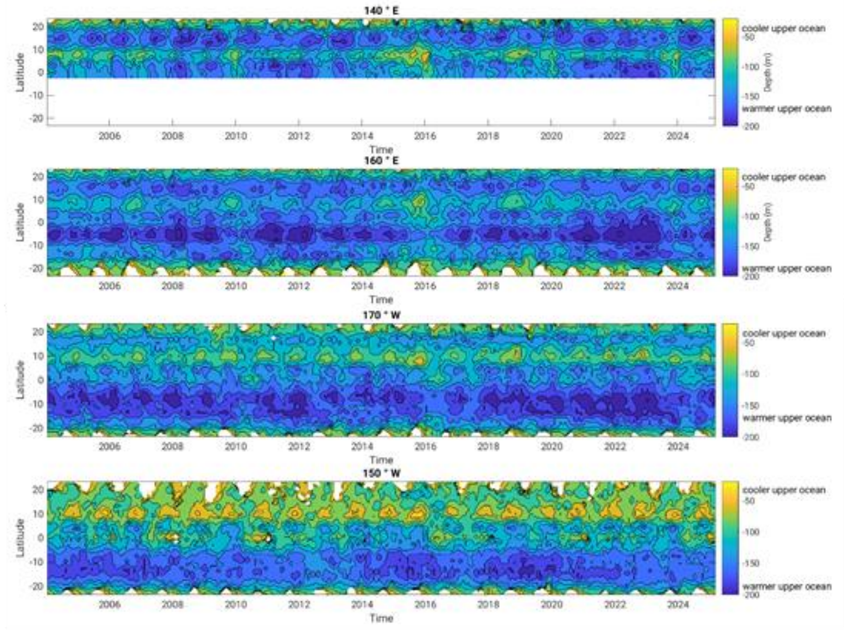

Figure A2-6: Timeseries of the depth (m) of the 24°C isotherm at 140°E, 160°E, 170°W (190°E) and 150°W (210°E) between 22.5°S and 22.5°N. The deeper the isotherm, the warmer the upper ocean.

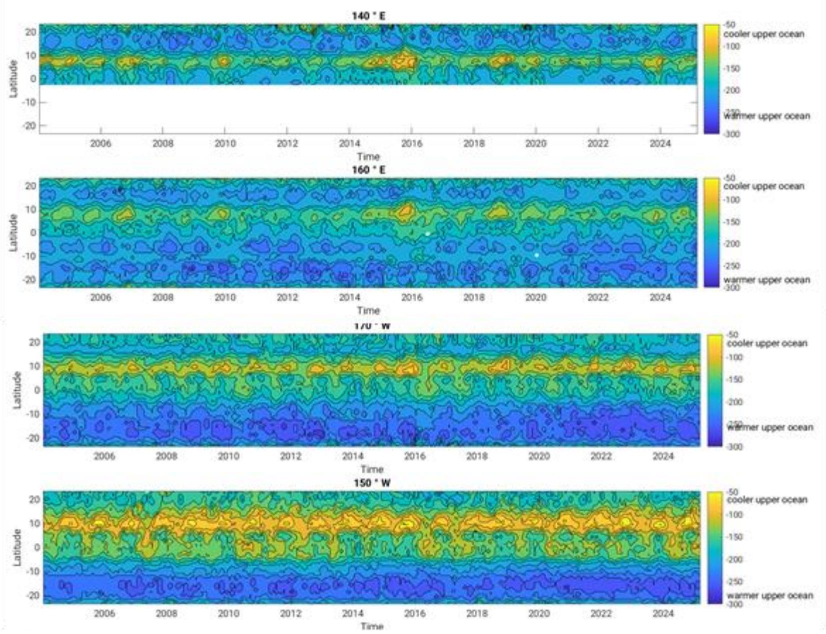

Figure A2-7: Timeseries of the depth (m) of the 20°C isotherm at 140°E, 160°E, 170°W (190°E) and 150°W (210°E) between 22.5°S and 22.5°N. The deeper the isotherm, the warmer the upper ocean.

WCPFC Climatological Indicators: Interdecadal Pacific Oscillation (IPO)

Description: The IPO is an oceanographic phenomenon influencing both the southern and northern Pacific. The period of oscillation is roughly 15–30 years. Positive phases of the IPO are characterized by a warmer than average tropical Pacific and cooler than average northern Pacific. Negative phases are characterized by an inversion of this pattern, with cool tropics and warm northern regions. The IPO had positive phases from 1922 to 1946 and 1978 to 1998, and a negative phase between 1947 and 1976.

The Tripole index for the IPO is based on the difference between the SST anomaly averaged over the central equatorial Pacific and the average of the SST anomaly in the northwest and southwest Pacific. The regions used to calculate the index are: Region 1: 25°N–45°N, 140°E–145°W, Region 2: 10°S–10°N, 170°E–90°W and Region 3: 50°S–15°S, 150°E–160°W. Data source: TPI filtered (IPO Tripole Index) of Henley et al. (2015) using ERSST V5 or COBE and created at NOAA PSL.

Status: The recent phases of IPO were: positive (1913–44), negative (1945–76), positive (1977–98) and negative from 1999. The IPO is currently expected to move into a positive phase. Reporting on IPO phase will assist WCPFC with understanding the rate of change in ocean dynamics (i.e. a positive phase may compound other equatorial warming). Current evaluation is that the IPO indicator meets all selection criteria. Development of this indicator is still underway.

WCPFC Climatological Indicators: El Niño Southern Oscillation (ENSO)

Description: The Oceanic Nino Index (ONI) tracks three-month averaged SST anomalies in the surface waters of the east-central tropical Pacific, near the International Dateline (i.e. between 120°-170°W) from a moving 30-year average temperature to identify El Nino or La Nina events. Index values of +0.5 or higher indicate El Nino, values of -0.5 or lower indicate La Nina. To be in an El Nino or La Nina state require both the ocean and atmosphere to be exhibiting synchronous behaviour.

ENSO shifts irregularly back and forth between El Nino and La Nina phases every two to seven years. Each phase triggers predictable disruptions of temperature, precipitation, and winds in the tropical Pacific Ocean. Easterly trade winds slow down (or may reverse) during El Nino which generates warmer-than-average waters in the central and eastern tropical Pacific. Rainfall increases in the central-east tropical Pacific and decreases in the western Pacific. La Nina has the opposite effect. The trade winds intensify during La Nina which generates cooler-than-average waters to the central and eastern tropical Pacific. Rainfall decreases in the central-east tropical Pacific and increases in the western Pacific. Neutral means neither El Nino nor La Nina conditions are present in both the ocean and the atmosphere. Sometimes "neutral" genuinely means that conditions in the ocean and the atmosphere are near average. If the conditions for El Nino or La Nina have been met in the ocean, but not in the atmosphere, this is also referred to as a neutral state.

Recent analyses of coral cores from the central Pacific Ocean provided evidence that El Nino intensity has increased in parallel with greenhouse gas emissions. Reporting on ENSO intensity and frequency will assist WCPFC with understanding the rate of change in equatorial dynamics (Figure A2-8). Given the influence of La Nina and El Nino events, seasonal forecasts (Figure A2-9) should aid WCPFC preparations for extreme events. The NOAA Global Climate Dashboard provides ready access to this information as does the Copernicus Marine Service. Current evaluation is that the ENSO indicator meets all indicator selection criteria.

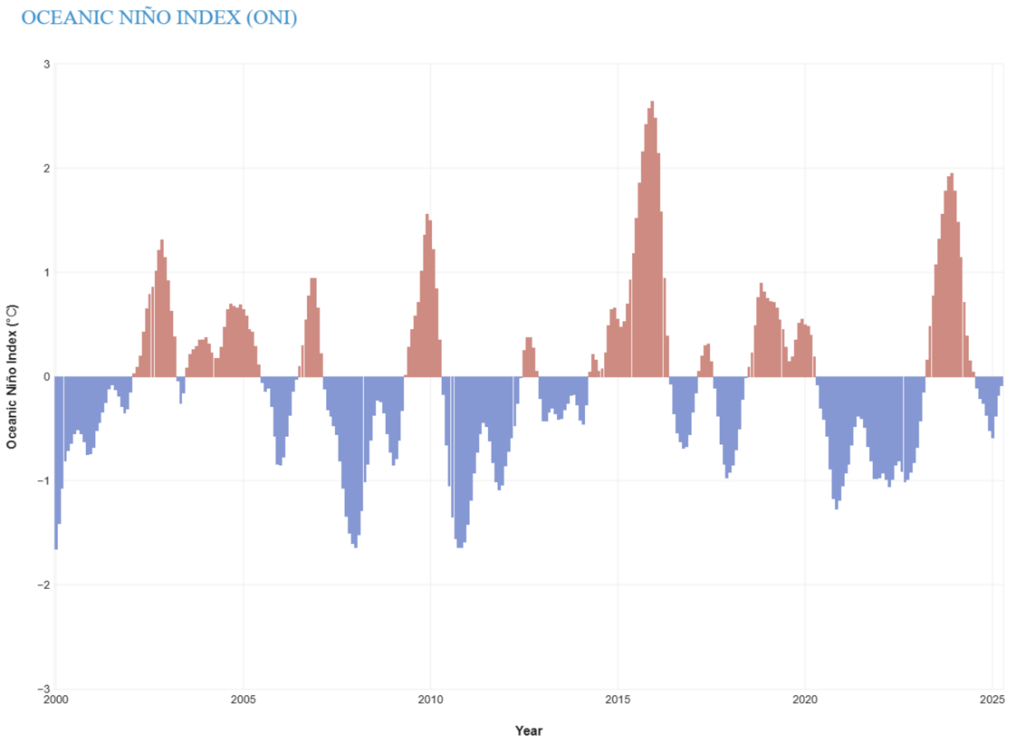

Figure A2-8: Example of the Oceanic Nino Index (Nino3.4) from 2000 to present (Source: NOAA Global Climate Dashboard).

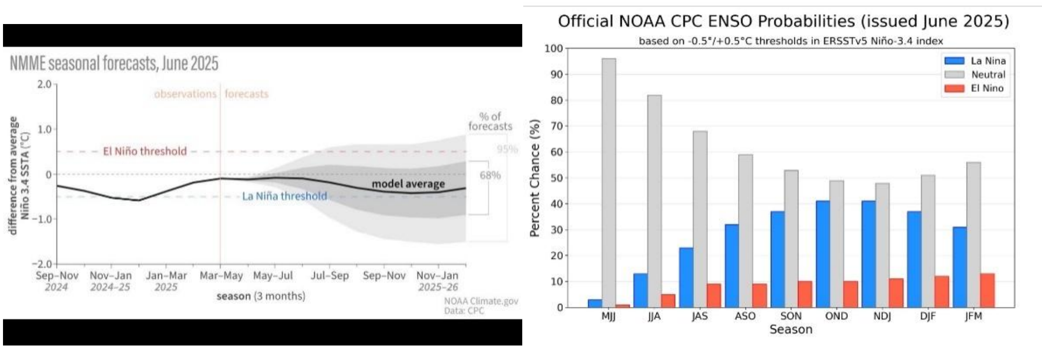

Figure A2-9: Examples of ENSO phase forecasting (Source: NOAA Global Climate Dashboard).

WCPFC Climatological Indicators: Marine Heatwaves

Description: Marine heat waves (MHW) are extreme rises in ocean temperature for an extended period of time. The total number of days with marine heatwaves, averaged over the entire globe, has increased by 50% over the last century and the number of marine heatwave events has doubled since 1982. Increases in the strength, frequency, and duration of marine heat waves are expected in the future due to climate change. Shifts in populations of marine species, mass mortality events including of non-mobile species, exacerbation of harmful algal blooms, and likelihood of extreme weather events can be expected with increases in MHWs.

Heatwave statistics and analysis follow those developed by Lal *et al.* 2025 (https://doi.org/10.5194/egusphere-2025-3281).

Status: Lal *et al*. 2025 examined MHWs in the south equatorial Pacific. Figure A2-10 shows the daily time series of the percentage of surface area of that region in a MHW state, for both GLORYS12 and NOAA-OISST. A significant trend of ~3.5 percent (~70 square degrees) increase per decade is observed (Figure A2-10). Over the past decade, there has not been a single day when at least part of the region was not exposed to a MHW. Lal *et al.* 2025 also provide a method for reporting on frequency, duration, and intensity (Figure A2-11). Current evaluation is that the MHW indicators of Lal *et al.* (2025) meet all indicator selection criteria.

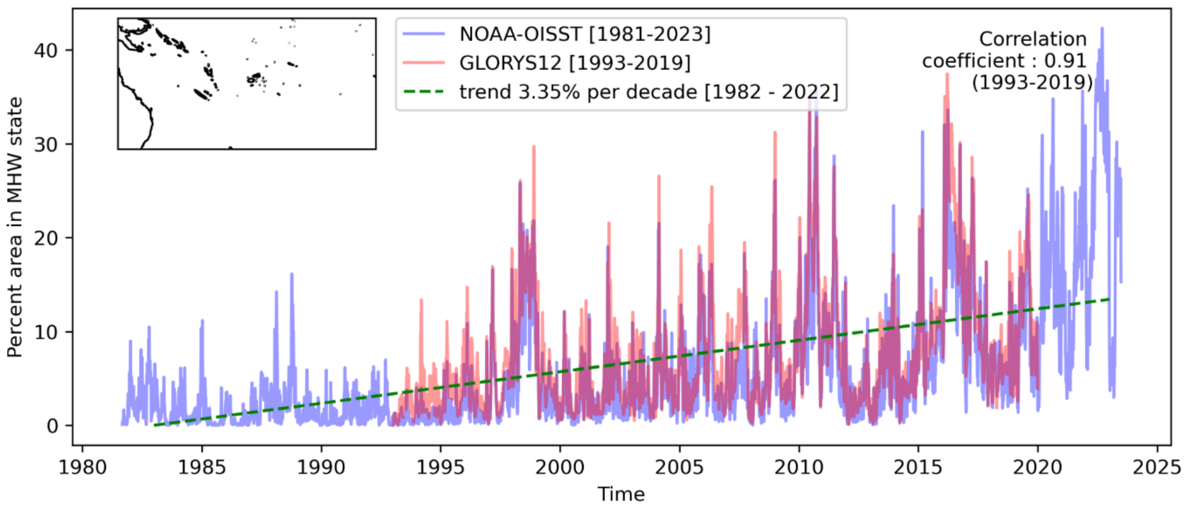

Figure A2-10: Timeseries showing percent of study region in MHW state, with a statistically significant trend line (p-value < 0.05) in green calculated between 1982 to 2022 for NOAA-OISST and Pearson correlation coefficient calculated between 1993 and 2019 for NOAA-OISST and GLORYS12 (p-value < 0.05). Source: Lal et al. 2025.

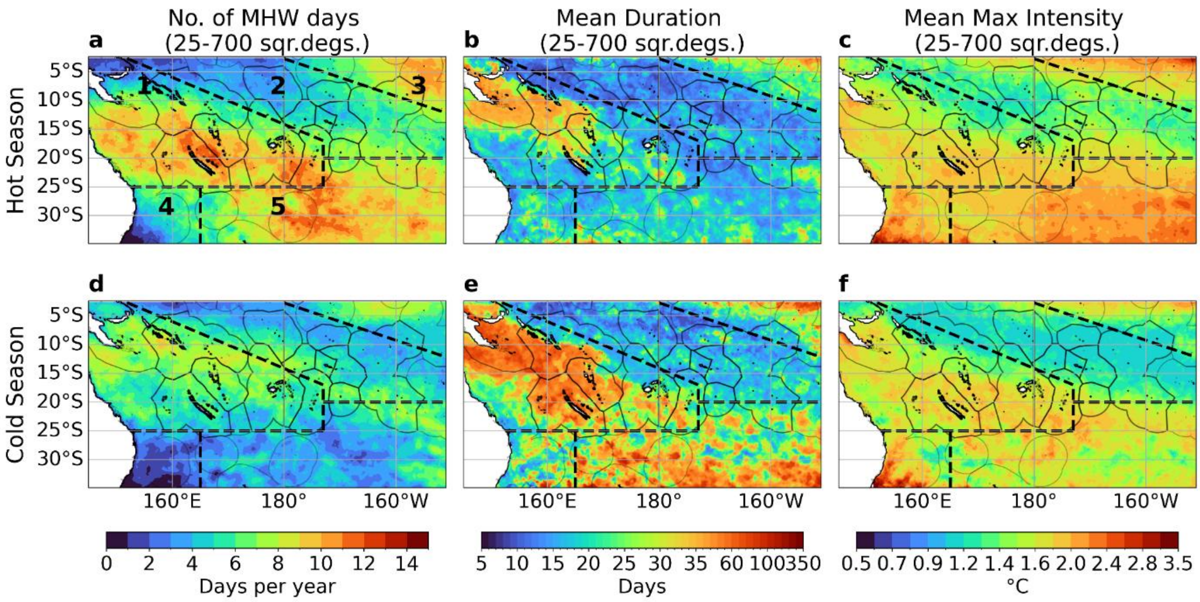

Figure A2-11: Panel plots showing number of MHW days, mean duration, and mean maximum intensity for macroscale events (25-700 square degrees); a,b,c in hot and d,e,f in cold season respectively. MHWs detected using NOAA-OISST from 1981-09 to 2023-06. Source: Lal et al. 2025.

Oceanographic Features/Regions: western Pacific warm pool

Description: The warm pool is a large, warm body of water at or above 28°C that sits in the equatorial WCPO. The warm pool naturally varies in size and extent, and in particular its longitudinal position varies with ENSO events. With the impacts of climate change, the warm pool is predicted to increase in size and volume, contributing to a potential eastward shift in tuna biomass (Bell *et al.,* 2021; Lehodey *et al.,* 2013). The warm pool is also considered as an important spawning ground for tuna species, in particular skipjack tuna and so changes in its size, structure or position may also influence the productivity of tuna (Ashida 2020; Fujioka *et al.,* 2024). Tracking the volume of the warm pool will provide an indicator of heat absorption and content of the WCPO.

Volume: The Roemmich and Gilson Argo climatology at 0.25° resolution was used to find the depth of the 28°C isotherm, which is used as a proxy for the volume of the western Pacific warm pool, at each spatial grid for each month. This indicator was calculated from 2004-2024 due to a step-change in data available as the Argo network came online in 2004.

Area: The ERA5 Atmospheric Reanalysis coupled to the NEMO ocean model was used to calculate changes in warm pool area. This model was chosen as it has been bias corrected and coupled with two climate change ESMs (as part of the next generation of SEAPODYM climate projections for tuna species), allowing for estimation of expected change in warm pool area under differing climate change scenarios.

Status: The depth and position of the warm pool is tracked across three longitudes spanning the WCPO region in an eastward direction at a monthly period from 2004-2024 using the 28°C isotherm depth as a proxy for volume (Figure A2-12). During El Nino events, an eastward movement of the warm pool is clearly seen with the extension and deepening of the 28°C isotherm along the equator at 170°W (190°E) and even at 150°W (210 °E). On the other hand, La Nina events are identified as a significant deepening of the 28°C isotherm at 160°E. In addition to ENSO, the volume of the warm pool shows both inter-annual and intra-annual variability. Extension of the warm pool volume in a north-south direction occurs at an annual period across the WCPO. The depth and off-equator extent of the warm pool volume shows significant variability. There has been a large north and south off-equatorial extension and deepening of the 28°C isotherm since 2024, particularly noticeable at 160°E and extending to 15°N. Noting this variability, this indicator is currently more suited to monitoring seasonal and inter-annual change rather than trends due to climate change.

The 29°C surface isotherm was used to calculate warm pool area (Figure A2-13). The area has trended positively to be outside two standard deviations of the historical mean and is tracking consistently with climate change projections. The warm pool area indicator departed from the detrended historical time series (i.e. ERA5 reanalysis detrended for greenhouse gas emissions) in the late 1970's. This indicator is suitable for WCPFC to use as a measure of climate change impact. Tracking the area of higher surface temperature isotherms (see Figure A2-14) is also recommended noting the results from Fujioka *et al.* 2024 showing increased mass mortality of egg and larvae of skipjack tuna at water temperatures greater than 31°C. Warm pool indicators meet all indicator selection criteria.

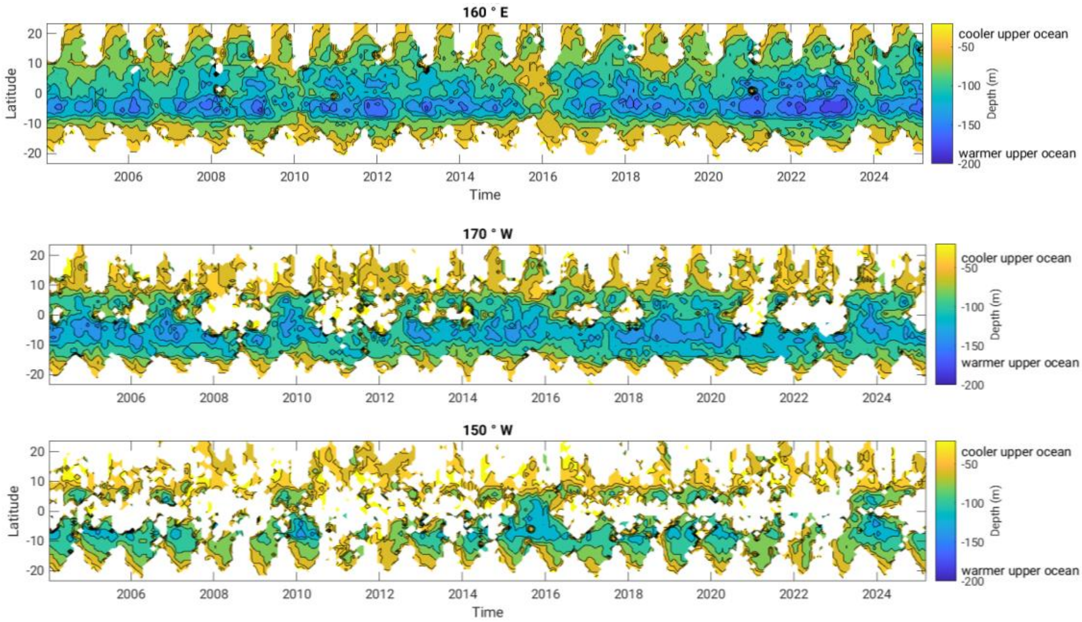

Figure A2-12: Timeseries of the depth (m) of the 28°C isotherm which is used as a proxy for warm pool volume at three longitudes: 160°E, 170°W (190°E) and 150°W (210°W) between 22.5°S and 22.5°N. The deeper the isotherm, the warmer the upper ocean.

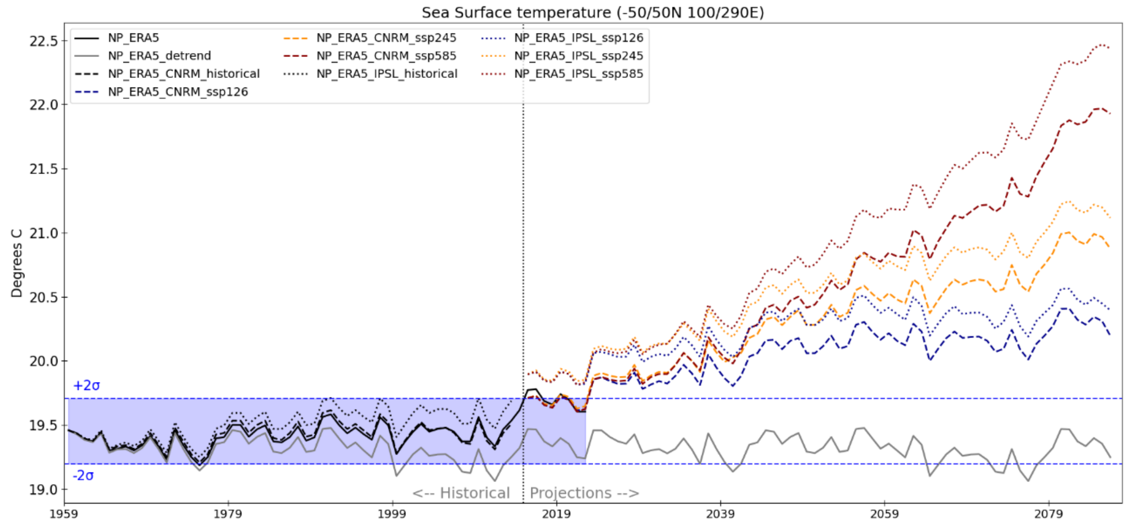

Figure A2-13: ERA5 atmospheric reanalysis coupled to NEMO measure timeseries of the area of the western Pacific warm pool using the 29°C surface temperature isotherm. Blue shaded is the ERA5 historical mean with two standard deviations. Grey solid line is the detrended ERA5 timeseries. Dashed lines are the projected climate scenarios from two ESM corrected for the ERA5 reanalysis.

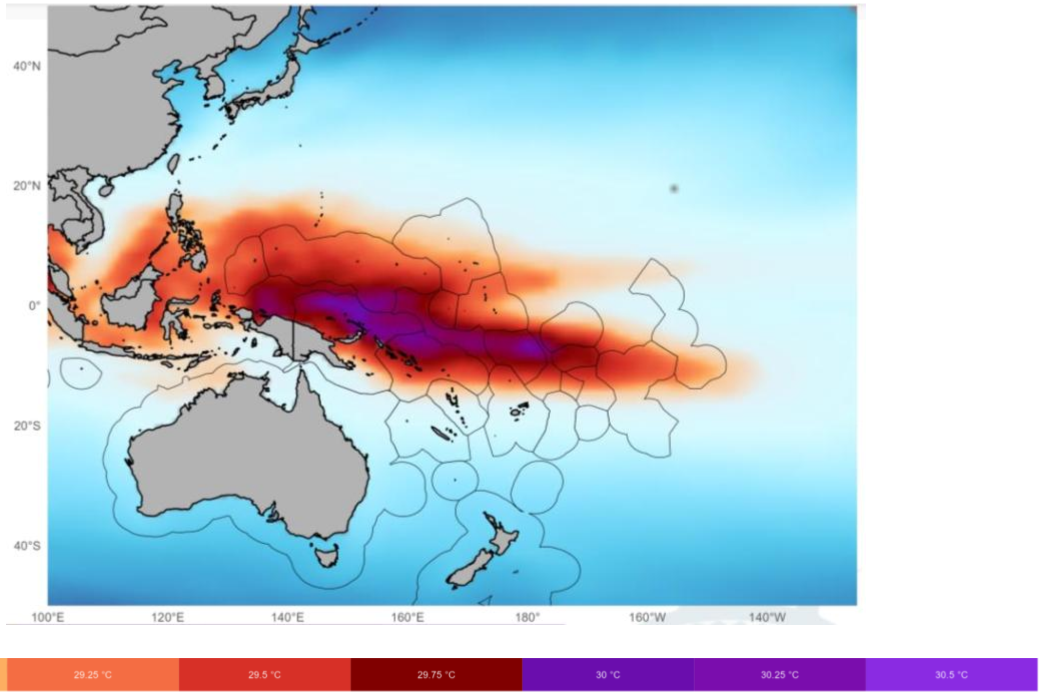

Figure A2-14: 2023 map of sea surface temperature isotherms in the western and central Pacific Ocean showing isotherms from 29-31.5°C.

Oceanographic Features/Regions: North and south Pacific gyres, Nino 3.4 region, Marine Heatwaves

These following indicators are still under development.

North and south Pacific gyres: Noting the long-term warming trends identified in the description of water temperatures it is recommended that the two regions representing the north Pacific gyre and south Pacific gyre are reported to WCPFC annually to track the rates of change.

Nino 3.4 region: It is recommended that seasonal forecasts are reported to WCPFC for advising on ENSO phase. Given the sensitivity detected in this region for trends in isotherm depth, reporting on this indicator will also aid interpretation of change in ocean heat content in this region.

Marine heatwaves: Given the increasing occurrence of MHW, reporting on their frequency, duration and intensity is recommended for two regions (equatorial and temperate) given the variability observed in SST and isotherm depth.

Noting that all these indicators meet the selection criteria.

Fishery Related: Surface chlorophyll-a concentration

Description: Chlorophyll-a concentration is a proxy for phytoplankton biomass, which constitutes the base of marine food webs. While tuna do not prey directly on phytoplankton, these primary producers support the dense aggregations of zooplankton and micronekton that are crucial prey fields for juvenile and adult tunas. Elevated concentrations of chlorophyll can be detected via satellite, much like sea surface temperature, and so enable a near-real time observational capacity. El Nino events have large impacts on chlorophyll concentrations, with substantial reductions across the WCPO, although these reductions are minimally offset by increases in the far west. Monitoring chlorophyll concentration is important as a proxy of phytoplankton biomass, productivity and thus prey availability. Climate models typically predict declines in tropical productivity in the coming decades associated with shifts in nutrient availability (Bopp *et al.,* 2005; Kwiatkowski *et al.,* 2020; Buchanan *et al.,* 2021; Buchanan *et al.,* 2025), although our confidence in these projections is low to moderate (Matear *et al.,* 2015; Tagliabue *et al.,* 2021).

This indicator was derived from the OCNET product from 2001-2023 (Hong *et al.,* 2023). This product leverages machine learning-based gap-filling to achieve near-global coverage. This product is at 0.25º degree horizontal resolution at a daily temporal resolution, which was regridded to a 1° degree horizontal resolution and monthly mean. The standard deviation of chlorophyll was calculated relative to the climatological mean across the timeseries. Figure A2-15 shows that chlorophyll concentrations have changed over the timeseries and that trends vary throughout the WCPO.

Status: Variations in chlorophyll are highest along coastlines and in the western equatorial Pacific between 150ºE-180ºE and 5ºS-5ºN (Figure A2-15). This patch of high variability in the western Pacific is a key area of tuna biomass and is directly affected by climate modes, in particular ENSO, making it prone to strong year-to-year fluctuations. However, this key region is also affected by the longer-term trends driven by climate change. Recent reports suggest that this patch of ocean has become more productive over the observational period (1997-2022), in direct contrast to widespread declines throughout the low latitude oceans, although it is still unclear whether this trend is due to anthropogenic climate change or natural variability (Silsbe *et al.,* 2025). It is

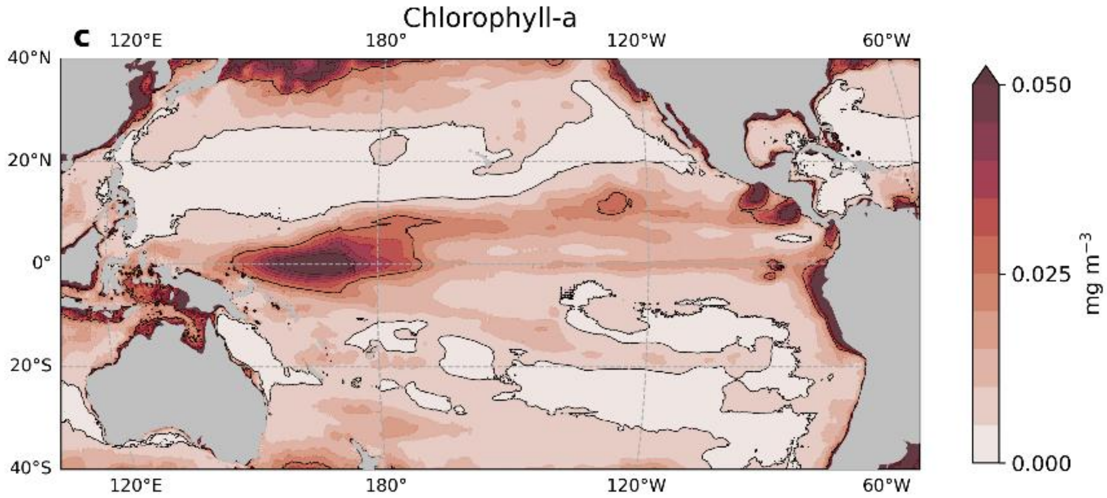

Figure A2-15: Monthly standard deviations in the surface concentration of chlorophyll from 2001-2023. Variations are relative to a climatological mean state, so that the values presented here can be interpreted as standard deviations from the mean.

recommended that this indicator is further developed before presentation to WCPFC.

Fishery Related: Oxygen Distribution and Concentration

Description: Dissolved oxygen is essential for pelagic predators like tuna with high metabolic demands. Some tropical tuna species make daily dives across large thermal and oxygen gradients. The typical behaviour of bigeye tuna, which dive deepest, is to remain at the surface during the night but forage within the mesopelagic (200-500m) during the day (Schaefer *et al.,* 2009). Mesopelagic waters, particularly in the Pacific, hold the lowest concentrations of dissolved oxygen, and as such bigeye tuna must periodically return to surface waters to reoxygenate (Schaefer & Fuller, 2010). Skipjack and yellowfin tuna, in contrast, forage in the warmer, well oxygenated surface waters and will only dive to forage when prey is depleted (Schaefer & Fuller, 2007; Schaefer *et al.,* 2011). Inter-annual variations and long-term trends in dissolved oxygen at the boundary to the mesopelagic zone are therefore important for controlling habitat suitability and foraging efficiency of tropical tuna species.

This indicator will be derived from the Gridded Ocean Biogeochemistry from Artificial Intelligence – Oxygen (GOBAI-O2) data product (Sharp *et al.,* 2023). This product is available for the period 2004-2023 and is updated yearly. GOBAI-O2 is a new four-dimensional gridded product of ocean interior oxygen, derived via machine learning algorithms trained on dissolved oxygen observations from Argo-float-mounted sensors and discrete measurements from ship-based surveys which are applied to temperature and salinity fields constructed from the global Argo array. GOBAI-O2 covers 86% of the global ocean area at a 1° resolution grid, from the sea surface to 2km depth.

Status: Interior dissolved oxygen concentrations across the tropical Pacific Ocean are declining (Schmidtko *et al.,* 2017) and are expected to continue declining as anthropogenic climate change drives increased stratification, a slowdown in ventilation via the upper overturning cell and losses in solubility (Oschlies *et al.,* 2018; Takano *et al.,* 2023; Kwiatkowski *et al.,* 2020). The low oxygen zones in the eastern Pacific have expanded in recent decades (Schmidtko *et al.,* 2017) and threaten ecosystem health and fisheries (Stramma *et al.,* 2021). While the climate-driven deoxygenation is supported by theory, observations and model projections, there is also substantial contributions to these trends via the modes of climate variations at interannual and decadal timescales, namely ENSO and IPO (Ito & Deutsch, 2013; Duteil *et al.,* 2018). Consequently, there is likely a high degree of decadal variability in mesopelagic dissolved oxygen across the WCPO that is yet to be fully appreciated in our short observational records. Noting these limitations, it is not recommended that this indicator is presented to WCPFC until methods are further developed toward producing an oxygen concentration indicator for the WCPO with associated understanding of the contributing components (decadal and longer term climate change contributions).

Fishery Related: Centre of gravity (COG) of the purse seine fishery

Description: The WCPFC purse seine fishery predominately operates in the western Pacific warm pool. The warm pool is a large, warm body of water at or above 28°C that sits in the equatorial WCPO. The warm pool naturally varies in size and extent, in particular with ENSO events, which influences where effort and catch consequently occurs in the purse seine fishery (Senina *et al.,* 2008). The warm pool is also considered as an important spawning ground for tuna species, in particular skipjack tuna and so changes in its size, structure or position may also influence the productivity of tuna (Ashida, 2020; Fujioka *et al.,* 2024). With the impacts of climate change, the warm pool is predicted to increase in size, influencing a potential eastward shift in tuna biomass (Bell *et al.,* 2021; Lehodey *et al.,* 2013). By monitoring the centre of gravity (COG) of purse seine effort and catch, we can potentially monitor if fisheries are responding to these predicted changes and by proxy tuna dynamics. Any shift in the location of the purse seine fishery is also relevant as it relates to income for PICTs when fishing occurs within their EEZ.

Tuna purse seine data, aggregated monthly by flag and set type, were extracted for the period 1990–2023 and constrained to the area between 15° S and 10° N latitude, and east of 130°E longitude. Flags with poor temporal coverage over the time period were excluded. The retained flags were FM, JP, KI, KR, PG, PH, SB, TW, US, VU. To explore spatial and temporal shifts in the longitude of fishing activity, generalized additive models (GAMs) were fitted in R (v. 4.5.0, R Core Team 2025) using the mcgv package (v.1.8-42; Wood 2017). All models assumed a Gamma distribution with a log link. All models were fit using the fast REML (method = "fREML") estimation routine and discrete = TRUE for computational efficiency given the large sample size (n ≈ 1.17 million). Nuisance variables with a fixed structure across all models explored were:

- month, modelled using a cyclic cubic spline to reflect the cyclic nature of year,
- latitude, modelled using a thin-plate spline to capture broad-scale spatial trends, and
- set-type (AFAD, DFAD, FREE) and Oceanic Nino Index (categorised into El Nino, La Nina, Neutral) were modelled as fixed effects.

We compared alternative model formulations to assess temporal trends (year, yy) and variation among fishing fleets (flags). See Table A2-1 for a description of each model fitted and its interpretation.

*Table A2-1: Summary of generalized additive model (GAM) structures explored. ^^ Shared smooth of year across flags, with flag-specific deviations (i.e., shared smoothing penalty). ** Separate smooths of year for each flag, estimated independently (i.e., no shared penalty).*

Name	Temporal model structure	Nuisance parameters
Linear	yy + s(flag, bs = 're', k = 10)	s(mm, k = 6, bs = 'cc') + set_type + oniF + s(latd, k=5)
Factor	yyF + s(flag, bs = 're', k = 10)	s(mm, k = 6, bs = 'cc') + set_type + oniF + s(latd, k=5)
Smooth	s(yy, k = 10) + s(flag, bs = 're')	s(mm, k = 6, bs = 'cc') + set_type + oniF + s(latd, k=5)
Year:flag shared smooth^^	s(yy, flag, bs = 'fs', k = 10)	s(mm, k = 6, bs = 'cc') + set_type + oniF + s(latd, k=5)
Year:flag separate smooths**	s(yy, by = flag, bs = 'fs')	s(mm, k = 6, bs = 'cc') + set_type + oniF + s(latd, k=5)

Status: Model comparison based on AIC, indicated strongest support for the model with a shared smooth of year per flag (year:flag shared smooth, Table A2-1), which explained 52.3% of the deviance and had the lowest AIC (Table A2-2). Based on this model, the marginal smooth of year averaged over all flags is shown in Figure A2-16. Flag-specific smooths are shown in Figure A2-17. The overall trend shows a westward shift in longitude from the early 1990s to around 2010, followed by a reversal with a progressive eastward movement. By the early 2020s, the average longitude had returned to approximately its original position, indicating a broad cyclical or looping spatial trend over time. Even when controlling for all nuisance parameters, the estimated magnitude of shift in longitude across years and flag is highly variable.

Table A2-2: Model comparison ranked by AIC, with deviance explained (dev).

	df	AIC	dAIC	pc.dev
mod_syearflag.sharedsmooth	112.010	8680908	0.00	0.523
mod.yyF.flag	55.998	8738461	57553.17	0.499
mod_syear_sflag	31.997	8823188	142280.05	0.462
mod_syearbyflag	203.335	8835423	154514.58	0.456
mod.yy.flag	23.998	8880115	199206.72	0.435

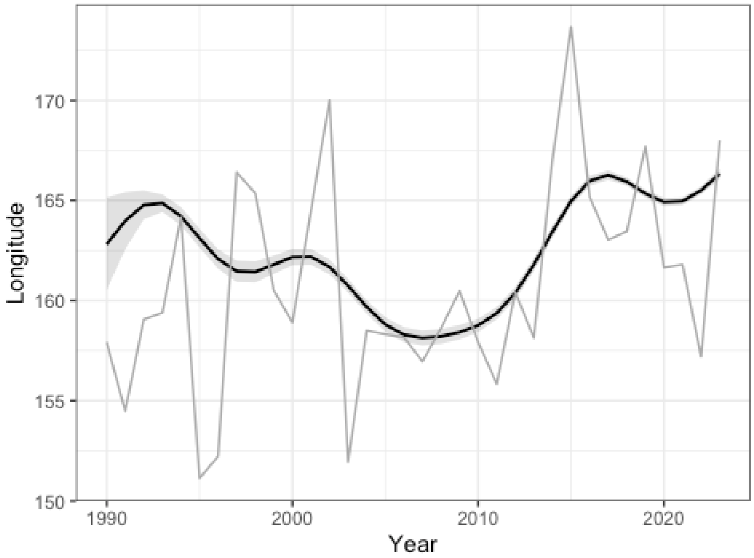

Figure A2-16: Marginal smooth of year averaged over all flags, based on the best fitting model. Average observed longitude for all flags by year is given in a dark grey line.

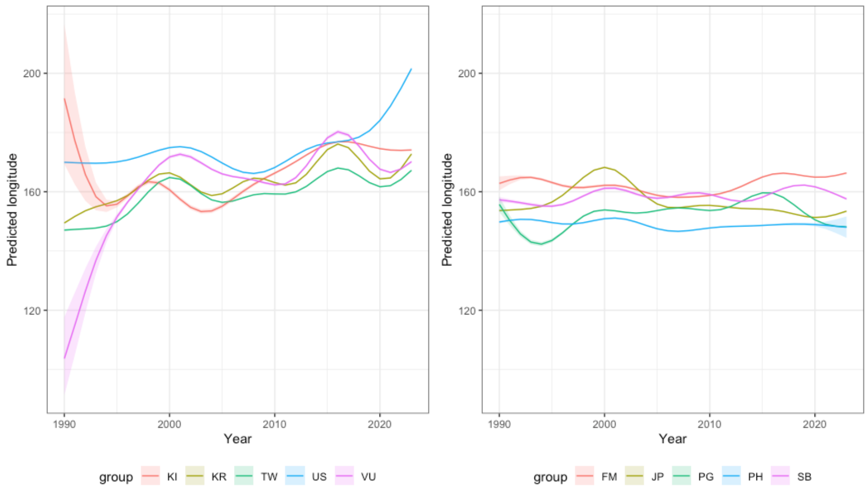

Figure A2-17: Flag-specific smooths of year with shared smoothing penalty based on the best model. Flags with increasing gradient over the time period (left hand panel) and flags with a stable gradient over the time period (right hand panel).

Model residuals in general are tolerable, but:

- Residuals on the response scale (i.e. longitude) showed deviations of up to ±30°, indicating substantial prediction error for some observations. While deviance residuals suggested the model was statistically consistent with the assumed error distribution, the magnitude of raw residuals highlights considerable uncertainty in spatial predictions and potential limitations in model structure or data coverage.

- Spatially, residuals are not great suggesting consistent under prediction of longitude in the west and over prediction of longitude in the east. Despite the spatial variables modelled here, it seems there is unaccounted spatial pattern in the data that flag and longitude are not accounting for.

It was apparent from this analysis that different flagged vessels behave differently within the fishery, with some flexibly fishing throughout the convention area while others consistently fish similar regions each year (Figure A2-17). This suggests that if climate change does affect the distribution of tuna, some vessels and flags will be more susceptible to these changes than others. However, currently it appears that COG cannot reliably detect a climate signal given the magnitude of inherent variability in the data and fishery due to other variables such as set type and flag. Therefore, this indicator may not meet criteria four from the SC12 criteria which requires the indicator to be responsive and with minimal time lags (Appendix 1).

Fishery Related: Size composition of tunas

Description: The size composition of a fish population is influenced by a range of factors including fishing and its environment. For example, changing oceanographic conditions could influence prey availability or recruitment having knock-on effects on fish size composition. How the environment and climate change is influencing tuna size composition is not well known currently.

To explore spatial and temporal shifts in the mean length of captured and measured fish, we fitted a suite of generalized additive models (GAMs) in R (v. 4.5.0, R Core Team 2025) using the mcgv package (v.1.8-42; Wood 2017). All models assumed a Gamma distribution with a log link, and the model was weighted by the number of fish measured to estimate each mean length. Nuisance variables with a fixed structure across all models explored were:

- quarter, modelled as a fixed effect, and
- a bivariate spatial smooth over latitude and longitude (5 degree spatial resolution), modelled using a tensor product.

We compared alternative model formulations to assess temporal trends (year, yy) and variation among fishing fleets (flags). See Table A2-3 for a description of each model fitted and its interpretation. Model comparison was based on AIC.

Table A2-3: *Summary of generalized additive model (GAM) structures explored. ^^ Shared smooth of year across flags, with flag-specific deviations (i.e., shared smoothing penalty). ** Separate smooths of year for each flag, estimated independently (i.e., no shared penalty).*

Name	Temporal model structure	Nuisance parameters
Null	s(flag, bs = ‘re’, k = 10)	qtrF + te(lat5, lon5, k = c(5, 10))
Linear	yy + s(flag, bs = ‘re’, k = 10)	qtrF + te(lat5, lon5, k = c(5, 10))
Factor	yyF + s(flag, bs = ‘re’, k = 10)	qtrF + te(lat5, lon5, k = c(5, 10))
Smooth	s(yy, k = 10) + s(flag, bs = ‘re’)	qtrF + te(lat5, lon5, k = c(5, 10))
Year:flag shared smooth^^	s(yy, flag, bs = ‘fs’, k = 10)	qtrF + te(lat5, lon5, k = c(5, 10))
Year:flag separate smooths**	s(yy, by = flag, bs = ‘fs’)	qtrF + te(lat5, lon5, k = c(5, 10))

Length data for skipjack tuna (SKJ) from the purse seine fishery were extracted for the period 1990–2023 and constrained to the area between 15° S and 10° N latitude, and east of 130°E longitude. Analysis based on individual lengths performed poorly, so mean length per 5° grid cell was used as the response variable. Temporal coverage of some flags were exceptionally sparse, so CK, NR, SU were removed.

Length data for bigeye (BET) and yellowfin tuna (YFT) from the longline fishery were extracted for the period 2000–2023. Temporal coverage of some flags were exceptionally sparse, so BZ, CK, GU, ID, KI, MH, NU, PG, PH, PW, SB, SU, TV, VN, VU, and WS were removed for BET and AU, BZ, ID, KI, MH, NU, NZ, PH, PW, SB, TV, VN, VU removed for YFT. Data were at 5° spatial resolution. Grid cells with fewer than 100 length measurements were omitted. Response variable was individual length of measured fish.

Table A2-4: Model comparison ranked by AIC, with deviance explained (dev).

Model	AIC	dev
Skipjack (SKJ)		
mod_syearbyflag	185181307	0.391
mod.yyF.flag	185322943	0.379
mod_syearflag.sharedsmooth	186240611	0.356
mod_syear_sflag	187452395	0.316
mod.yy.flag	188079286	0.295
mod_null	188325990	0.286
Bigeye (BET)		
mod_syearbyflag	32693675	0.262
mod_syearflag.sharedsmooth	32697971	0.261
mod.yyF.flag	32742275	0.251
mod_syear_sflag	32754803	0.248
mod.yy.flag	32789008	0.240
mod_null	32795668	0.238
Yellowfin (YFT)		
mod_syearflag.sharedsmooth	22842749	0.203
mod_syearbyflag	22904914	0.183
mod.yyF.flag	22900330	0.183
mod_syear_sflag	22922717	0.175
mod.yy.flag	22936454	0.170
mod_null	22937150	0.169

Status: The model with the highest deviance explained was mod_syearbyflag for SKJ (39.1%, Table A2-4), mod_syearbyflag for BET (26.2%, Table A2-4) and mod_syearflag.sharedsmooth for YFT (20.3%, Table A2-4). Although these models were the best performing of those explored, uncertainty in model fits remained unsatisfactorily high. Prediction in mean length uncertainty spanned 40cm (i.e., 50% of the observed mean lengths) for SKJ, 120cm for BET and 100cm for YFT, representing substantial uncertainty.

Trends in the size composition of tunas has varied from 1990-2024 and there are no clear trends. This is likely a reflection of several factors including changes in sampling design, fishing strategy, and the underlying environment and populations. There is no evidence of an underlying climate trend in the length composition of tunas over time. It remains difficult to disentangle a range of variables that are likely to influence the size composition of tunas sampled such as the resolution and robustness of input data, changes in fishing pressure and strategy, natural environmental variability and so on. Further, empirical length indicators are generally not considered responsive to population level shifts in abundance and thus are not likely to be an appropriate indicator. It is unlikely that this indicator can reliably detect a climate signal and therefore, may not meet criteria four from the SC12 criteria which requires the indicator to be responsive and with minimal time lags (Appendix 1).